Available online at www.sciencedirect.com

ScienceDirect

IFAC Papers Online CONFERENCE PAPER ARCHIVE

IFAC-PapersOnLine 48-12 (2015) 370–375

Connected Vehicle Systems with Nonlinear Dynamics and Time Delays

Linjun Zhang and Gábor Orosz

Department of Mechanical Engineering, University of Michigan, Ann Arbor, MI, 48105, USA (e-mail: linjunzh@umich.edu, orosz@umich.edu).

Abstract: In this paper, we investigate the nonlinear dynamics of connected vehicle systems in presence of time delays, which may arise due to human reaction time and/or due to intermittency and packet drops in wireless communication. Stability conditions are derived by using the Lyapunov-Krasovskii theory. A generalized frequency response function is also developed to characterize the input-output response of nonlinear vehicle networks. Numerical simulations are used to validate the analytical results.

Keywords: Time delay, nonlinearity, vehicle-to-vehicle communication, networks, string stability

1. INTRODUCTION

Research on cooperative adaptive cruise control (CACC) has been receiving increasing attention due to the great potentials of wireless vehicle-to-vehicle (V2V) communication in improving traffic efficiency; see Milanes et al. (2014); Zhao et al. (2014); Ploeg et al. (2014). CACC refers to a platoon of vehicles where all vehicles react to the motion of the vehicle immediately ahead based on information obtained by range sensors (e.g., radar) while also monitoring the motion of the designated leading vehicle via V2V communication. However, implementing CACC in real traffic is difficult since it requires that radar-equipped vehicles follow each other, which rarely occurs in the real world due to the low penetration of such vehicles. Moreover, the requirement that each vehicle should communicate with the leader limits the length of platoon due to the effective communication range.

To relax the constraints above, connected cruise control (CCC) was proposed by Zhang and Orosz (2013); Orosz (2014), which utilizes information broadcasted by multiple vehicles ahead. CCC requires no prescribed leader and allow the incorporation of vehicles that are not equipped with range sensors and/or communication devices. Mixing CCC vehicles into traffic flow leads to connected vehicle systems (CVSs) that are implementable in practice while the enhanced flexibility increases the design complexity. Zhang and Orosz (2015a) and Ge and Orosz (2014) studied the dynamics the CVSs by using the linearized model so that the results were only valid in the vicinity of the equilibrium. Zhang and Orosz (2015b) investigated nonlinear dynamics of a class of delayed CVSs where all vehicles only monitor the motion of the vehicle immediately ahead. In this paper, we extend the analysis to CVSs where CCC vehicles monitor multiple vehicles ahead. Stability conditions are derived based on the Lyapunov-Krasovskii theory. We also study the frequency response of CVSs to evaluate their robustness against disturbances arising from vehicles ahead.

⋆ This work was supported by the National Science Foundation (Award Number 1351456).

2. CONNECTED CRUISE CONTROL

In Fig. 1, the CCC vehicle i (red) monitors the position s_j and the velocity v_j of vehicles $j = p, \dots, i-1$. The symbol l_j denotes the length of vehicle j. The long links can only be realized by wireless communication and the delay $\sigma \approx 0.2$–0.4 [s] arises due to intermittency and packet drops; see Qin et al. (2014). The short link can be realized using communication with $\xi = \sigma$, through human perception with human reaction time $\xi \approx 0.5$–2 [s] (Johansson and Rumar (1971)), or by range sensors (e.g., radar) with sensing delay $\xi \approx 0.1$–0.2 [s].

In this paper, we neglect the air-drag and the rolling resistance in the physics-based model presented in Orosz (2014). Then, the acceleration of vehicle i is determined by the controller:

$$\begin{aligned}\dot{s}_i(t) &= v_i(t)\,,\\ \dot{v}_i(t) &= \alpha_1\big(V\big(h_{i,i-1}(t-\xi)\big) - v_i(t-\xi)\big)\\ &\quad + \beta_1\big(v_{i-1}(t-\xi) - v_i(t-\xi)\big)\\ &\quad + \sum_{j=p}^{i-2} \alpha_{i-j}\big(V_i\big(h_{i,j}(t-\sigma)\big) - v_i(t-\sigma)\big)\\ &\quad + \sum_{j=p}^{i-2} \alpha_{i-j}\big(v_j(t-\sigma) - v_i(t-\sigma)\big)\,,\end{aligned} \tag{1}$$

where the constants α_{i-j} and β_{i-j} are control gains along the links of "length" $i-j$; see Fig. 1. The quantity

$$h_{i,j}(t) = \frac{1}{i-j}\left(s_j(t) - s_i(t) - \sum_{k=j}^{i-1} l_k\right) \tag{2}$$

denotes the average distance between vehicles i and j. Such averaging is used to make the equilibrium independent of the network size. Moreover, $V(h)$ denotes the range policy function that gives the desired speed as a function of h. Here, we use the nonlinear range policy function

$$V(h) = \begin{cases} 0\,, & \text{if } h \le h_{\rm st}\,,\\ \dfrac{v_{\max}}{2}\left[1 - \cos\left(\pi\dfrac{h-h_{\rm st}}{h_{\rm go}-h_{\rm st}}\right)\right], & \text{if } h_{\rm st} < h < h_{\rm go}\,,\\ v_{\max}\,, & \text{if } h \ge h_{\rm go}\,,\end{cases} \tag{3}$$

Peer review under responsibility of International Federation of Automatic Control.
10.1016/j.ifacol.2015.09.406

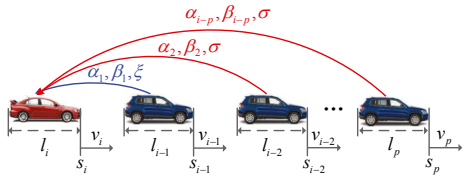

Fig. 1. A CCC vehicle (red) monitors the motion of multiple vehicles ahead. The short link (blue) can be realized by human perception, range sensors, or communication, thus the delay ξ can be human reaction time, sensing delay, or communication delay, respectively. Long links (red) can only be realized via wireless communication with delay σ. Symbols s_j, l_j, and v_j denote the position, length, and velocity of vehicle j, respectively, while α_{i-j},β_{i-j} are control gains for the link of "length" $i-j$.

which indicates that the vehicle tends to stop for small distances and aims to maintain the preset maximum speed $v_{\max}$ for large distances. In the middle, the desired velocity monotonically increases with the distance. The nonlinearity in (3) ensures the smooth change of acceleration at $h = h_{\rm st}$ and $h = h_{\rm go}$ and hence improves the driving comfort. According to the data collected in real traffic (Orosz et al. (2010)), parameters in (3) are set to be $h_{\rm st} = 5$ [m], $h_{\rm go} = 35$ [m], $v_{\max} = 30$ [m/s].

We remark that the CCC framework (1) guarantees the existence of a unique uniform flow equilibrium

$$s_i^*(t) = v^* t - i h^* - \sum_{k=0}^{i-1} l_k\,, \quad v_i(t) \equiv v^* = V(h^*)\,, \qquad (4)$$

for all i, which is independent of network size, connectivity structures, information delays, and control gains. The constant h^* denotes the equilibrium distance between any pair of consecutive vehicles while the constant v^* is the equilibrium velocity.

3. STABILITY OF CONNECTED VEHICLE SYSTEMS

To evaluate the stability, we use the perturbations

$$\tilde{s}_i(t) = s_i(t) - s_i^*(t)\,, \quad \tilde{v}_i(t) = v_i(t) - v^* \qquad (5)$$

about the equilibrium (4). To characterize the performance of CVSs, we evaluate *plant stability* and *head-to-tail string stability*. A vehicle i is said to be plant stable if it approaches the equilibrium in absence of perturbations from vehicles ahead. That is, if $\tilde{s}_j(t) \equiv 0$, $\tilde{v}_j(t) \equiv 0$ for $j = 0, \ldots, i-1$, then

$$\tilde{s}_i(t) \to 0\,, \quad \tilde{v}_i(t) \to 0\,, \quad \text{as } t \to \infty\,. \qquad (6)$$

A vehicle network is said to be plant stable if all following vehicles approach the equilibrium when the leading vehicle moves at a constant speed. We remark that, for linear time-invariant systems where the stability can be guaranteed globally, the plant stability of all following vehicles is a necessary and sufficient condition for the plant stability of the vehicle network. However, for nonlinear systems, plant stability of all vehicles is only a necessary condition for the plant stability of the network.

When certain vehicles cause disturbances, these disturbances propagate upstream along the network. For an $(n+1)$-vehicle network where the head and the tail vehicles are indexed by 0 and n, respectively, the head-to-tail string stability requires that, in steady state, the vehicle n attenuates the disturbances arising from vehicle 0, i.e.,

$$\|\tilde{v}_{ns}\| \le \|\tilde{v}_0\|\,, \qquad (7)$$

where the subscript "s" denotes the steady state. Indeed, the definition of head-to-tail string stability is particularly useful for vehicle networks containing human-driven vehicles, of which the dynamics cannot be designed and hence may amplify disturbances. The magnitude of disturbances can be evaluated by $\mathcal{L}_2$ norm (Ploeg et al. (2014)), which characterizes the "energy" of the disturbance signal. Since in practice the peak value of the disturbance may be more relevant, we use the $\mathcal{L}_\infty$ norm that is defined by $\|\tilde{v}\|_\infty = \sup_{t>0} |\tilde{v}(t)|$.

Substituting (5) into (1) yields

$$\begin{aligned}
\dot{\tilde{s}}_i(t) &= \tilde{v}_i(t)\,,\\
\dot{\tilde{v}}_i(t) &= \alpha_1\big(V(h_{i,i-1}(t-\xi)) - V(h^*) - \tilde{v}_i(t-\xi)\big)\\
&\quad + \beta_1\big(\tilde{v}_{i-1}(t-\xi) - \tilde{v}_i(t-\xi)\big)\\
&\quad + \sum_{j=p}^{i-2} \alpha_{i-j}\big(V(h_{i,j}(t-\sigma)) - V(h^*) - \tilde{v}_i(t-\sigma)\big)\\
&\quad + \sum_{j=p}^{i-2} \beta_{i-j}\big(\tilde{v}_j(t-\sigma) - \tilde{v}_i(t-\sigma)\big)\,.
\end{aligned} \qquad (8)$$

We assume that the distance between each pair of consecutive vehicles is always bounded, that is, $h_{k,k-1} \in \mathcal{D} \subseteq \mathbb{R}_+$ for $k = 1, 2, \ldots$. It follows that $h^* \in \mathcal{D}$ and $h_{i,j} \in \mathcal{D}$ for all $i, j = 1, 2, \ldots$; cf. (2). Since the function $V(h)$ in (3) is continuously differentiable for all h, based on the mean value theorem, there exist variables $\psi_{i,j} \in \mathcal{D}$, such that

$$V(h_{i,j}(t-\xi)) - V(h^*) = \frac{V'(\psi_{i,j})}{i-j}(\tilde{s}_j(t-\xi) - \tilde{s}_i(t-\xi))\,, \qquad (9)$$

cf. (2), where the prime denotes the derivative with respect to the headway h. We remark that, $\psi_{i,j}$ depends on $h_{i,j}(t-\xi)$ and h^* but it does not depend on time t explicitly, and $\psi_{i,j}$ is always bounded by the compact domain $\mathcal{D}$. Since $V'(h)$ is continuous with respect to h (cf. 3), $V'(\psi_{i,j})$ is also bounded for $\forall \psi_{i,j} \in \mathcal{D}$.

Defining $\tilde{x}_i(t) = [\tilde{s}_i(t)\,, \tilde{v}_i(t)]^{\rm T}$, substituting (9) into (8), and writing the result into matrix form, we obtain

$$\begin{aligned}
\dot{\tilde{x}}_i(t) &= A_0 \tilde{x}_i(t) + A_{\xi,i}(\Psi_i)\tilde{x}_i(t-\xi) + A_{\sigma,i}(\Psi_i)\tilde{x}_i(t-\sigma)\\
&\quad + B_1(\Psi_i)\tilde{x}_{i-1}(t-\xi) + \sum_{j=p}^{i-2} B_{i-j}(\Psi_i)\tilde{x}_j(t-\sigma)\,,
\end{aligned} \qquad (10)$$

where $\Psi_i = \big[\psi_{i,i-1}, \ldots, \psi_{i,p}\big]$ and other matrices are given by

$$\begin{aligned}
A_0 &= \begin{bmatrix} 0 & 1 \\ 0 & 0 \end{bmatrix}\,, \quad A_{\xi,i}(\Psi_i) = \begin{bmatrix} 0 & 0 \\ -\varphi_1(\psi_{i,i-1}) & -\kappa_1 \end{bmatrix}\,,\\
A_{\sigma,i}(\Psi_i) &= \begin{bmatrix} 0 & 0 \\ -\sum_{k=p}^{i-2}\varphi_{i-k}(\psi_{i,k}) & -\sum_{k=p}^{i-2}\kappa_{i-k} \end{bmatrix}\,,\\
B_{i-k}(\Psi_i) &= \begin{bmatrix} 0 & 0 \\ \varphi_{i-k}(\psi_{i,k}) & \beta_{i-k} \end{bmatrix}\,,
\end{aligned} \qquad (11)$$

for $j = p, \ldots, i-1$ and

$$\varphi_{i-j}(\psi_{i,j}) = \frac{\alpha_{i-j} V'(\psi_{i,j})}{i-j}\,, \quad \kappa_{i-j} = \alpha_{i-j} + \beta_{i-j}\,. \qquad (12)$$

Note that (10) is equivalent to (1) as no approximation is used during the derivation. To save space, we will not spell out the argument $\psi_{i,j}$ in $\varphi_{i,j}(\psi_{i,j})$ and the argument Ψ_i in $A_{\xi,i}(\Psi_i)$, $A_{\sigma,i}(\Psi_i)$, and $B_{i-k}(\Psi_i)$ in the rest of this paper.

3.1 Plant Stability

First, we define two matrices that will be used in the plant stability conditions

$$A_i = A_0 + A_{\xi,i} + A_{\sigma,i}\,, \quad A_{\mathrm{d},i} = A_{\xi,i} + A_{\sigma,i}\,, \tag{13}$$

cf. (11). Then, for cases $\xi = \sigma$ and $\xi \neq \sigma$, sufficient stability conditions are presented in Theorem 1 and Theorem 2, respectively.

Theorem 1. When $\xi = \sigma$, vehicle i is plant stable if for all $h_{i,j} \in \mathcal{D}\,(j = i-1,\dots,p)$ there exist positive definite matrices P, Q, W such that

$$\Omega = \begin{bmatrix} \dfrac{G}{\sigma} & A_0^{\mathrm{T}} W A_{\mathrm{d},i} & -P A_{\mathrm{d},i} \\ A_{\mathrm{d},i}^{\mathrm{T}} W A_0 & \dfrac{\sigma A_{\mathrm{d},i}^{\mathrm{T}} W A_{\mathrm{d},i} - Q}{\sigma} & \mathbf{0}_{2\times 2} \\ -A_{\mathrm{d},i}^{\mathrm{T}} P & \mathbf{0}_{2\times 2} & -W \end{bmatrix} \tag{14}$$

is negative definite over the domain $\mathcal{D}^{i-p}$, where

$$G = {A_i}^{\mathrm{T}} P + P A_i + Q + \sigma A_0^{\mathrm{T}} W A_0\,. \tag{15}$$

Note that the domain $\mathcal{D}^{i-p}$ include all possible values of Ψ_i.

Theorem 2. When $\xi \neq \sigma$, vehicle i is plant stable if for all $h_{i,j} \in \mathcal{D}\,(j = i-1,\dots,p)$ there exist positive definite matrices P, Q_1, Q_2, W_1, W_2 and an appropriate matrix R such that

$$\Xi_1 = \begin{bmatrix} \dfrac{H_2}{\sigma} & \dfrac{A_0^{\mathrm{T}} H_1 A_{\xi,i}}{\sigma} & \dfrac{A_0^{\mathrm{T}} H_1 A_{\sigma,i}}{\sigma} & -P A_{\mathrm{d},i} \\ \dfrac{A_{\xi,i}^{\mathrm{T}} H_1 A_0}{\sigma} & \dfrac{A_{\xi,i}^{\mathrm{T}} H_1 A_{\xi,i} - Q_1}{\sigma} & \dfrac{A_{\xi,i}^{\mathrm{T}} H_1 A_{\sigma,i}}{\sigma} & \mathbf{0}_{2\times 2} \\ \dfrac{A_{\sigma,i}^{\mathrm{T}} H_1 A_0}{\sigma} & \dfrac{A_{\sigma,i}^{\mathrm{T}} H_1 A_{\xi,i}}{\sigma} & \dfrac{A_{\sigma,i}^{\mathrm{T}} H_1 A_{\sigma,i} - Q_2}{\sigma} & \mathbf{0}_{2\times 2} \\ -A_{\mathrm{d},i}^{\mathrm{T}} P & \mathbf{0}_{2\times 2} & \mathbf{0}_{2\times 2} & -W_1 \end{bmatrix}, \quad \Xi_2 = \begin{bmatrix} -R & -\mathrm{sgn}(\xi-\sigma) P A_{\sigma,i} \\ -\mathrm{sgn}(\xi-\sigma) A_{\sigma,i}^{\mathrm{T}} P & -W_2 \end{bmatrix} \tag{16}$$

are negative definite over the domain $\mathcal{D}^{i-p}$, where

$$\begin{aligned} H_1 &= \sigma W_1 + |\xi-\sigma| W_2\,, \\ H_2 &= P A_i + A_i^{\mathrm{T}} P + Q_1 + Q_2 + A_0^{\mathrm{T}} H_1 A_0 + |\xi-\sigma| R\,. \end{aligned} \tag{17}$$

Theorem 1 was proved in Zhang and Orosz (2015b) while the proof of Theorem 2 is given in Appendix A. Recall that the matrices $A_{\xi,i}$ and $A_{\sigma,i}$ depend on the state; cf. (9) and (11). But the explicit expressions of $\psi_{i,j}$ are not needed. When applying these two theorems, we begin with discretizing the domain $\mathcal{D}^{i-p}$, and then solve the linear matrix inequalities (LMIs) numerically for P, Q, W in Theorem 1 or for P, Q_1, Q_2, W_1, W_2, R in Theorem 2 by using LMI package in Matlab. We remark that there may exist multiple solutions but we stop the calculation when a solution is found.

3.2 Head-to-Tail String Stability

To evaluate head-to-tail string stability, we investigate the steady-state response of the corresponding nonlinear delayed network under periodic disturbance. A sufficient condition for the existence of periodic steady-state response is provided in the following theorem.

Theorem 3. Suppose that the disturbance imposed on the head vehicle is T-periodic. If Theorem 1 and Theorem 2 hold for cases $\xi = \sigma$ and $\xi \neq \sigma$, respectively, then the vehicle network has T-periodic steady-state response, i.e.,

$$\tilde{x}_{i\mathrm{s}}(t+T) = \tilde{x}_{i\mathrm{s}}(t)\,, \quad i = 1, 2, \dots \tag{18}$$

where the subscript "s" represents the steady state.

The proof of Theorem 3 is given in Appendix B. Theorem 3 implies that a periodic excitation leads to a periodic steady-state response with the same period. Here, we investigate the frequency response of CVSs by imposing the sinusoidal disturbance

$$\tilde{s}_0(t) = \frac{v_{\mathrm{amp}}}{\omega}\sin(\omega t)\,, \quad \tilde{v}_0(t) = v_{\mathrm{amp}}\cos(\omega t) \tag{19}$$

on the head vehicle 0; cf. (5), where $v_{\mathrm{amp}}\,, \omega \in \mathbb{R}_+$ denote the amplitude and the frequency of the disturbance, respectively. Since $\tilde{s}_0(t)$ and $\tilde{v}_0(t)$ are periodic with period $T = 2\pi/\omega$, according to Theorem 3, the steady-state response of this vehicle network has the same period. However, due to the nonlinear dynamics, the steady states are not purely sinusoidal but may be expressed by using the Fourier series.

Considering (7) and (19), a vehicle network is head-to-tail string stable for amplitude v_{amp} if the head-to-tail amplification ratio satisfies

$$\Phi_{n,0}(\omega, v_{\mathrm{amp}}) = \|\tilde{v}_{n\mathrm{s}}\|/\|\tilde{v}_0\| < 1 \tag{20}$$

for all $\omega > 0$. This condition is different from those used for linear networks, where the amplification ratio only depends on the disturbance frequency ω; see Zhang and Orosz (2013).

To apply condition (20), the steady-state velocity of the tail vehicle needs to be determined. However, the analytical expressions may not be obtained in a closed form due to nonlinearities and delays. Thus, we seek for the approximations by using the third-order Taylor expansion of (1) about the uniform flow equilibrium (4), which yields

$$\begin{aligned} \dot{\tilde{s}}_i(t) &= \tilde{v}_i(t)\,, \\ \dot{\tilde{v}}_i(t) &= -\varphi_1^* \tilde{s}_i(t-\xi) - \kappa_1 \tilde{v}_i(t-\xi) \\ &\quad + \varphi_1^* \tilde{s}_{i-1}(t-\xi) + \beta_1 \tilde{v}_{i-1}(t-\xi) \\ &\quad + \alpha_1 \sum_{q=2}^{3} \epsilon_q \big(\tilde{s}_{i-1}(t-\xi) - \tilde{s}_i(t-\xi)\big)^q \\ &\quad + \sum_{j=p}^{i-2} \Big[-\varphi_{i-j}^* \tilde{s}_i(t-\sigma) - \kappa_{i-j} \tilde{v}_i(t-\sigma) \\ &\qquad + \varphi_{i-j}^* \tilde{s}_j(t-\sigma) + \beta_{i-j} \tilde{v}_j(t-\sigma) \\ &\qquad + \alpha_{i-j} \sum_{q=2}^{3} \epsilon_q \Big(\frac{\tilde{s}_j(t-\sigma) - \tilde{s}_i(t-\sigma)}{i-j} \Big)^q \Big]\,, \end{aligned} \tag{21}$$

where $\varphi_{i-j}^* = \varphi_{i-j}(h^*)$ and κ_{i-j} are given in (12), and $\epsilon_q = \frac{1}{q!}\frac{\mathrm{d}^q V(h^*)}{\mathrm{d}h^q}$ for $q = 2, 3$.

The solutions of (21) can be expressed as $\tilde{s}_i(t, \epsilon_2, \epsilon_3)$ and $\tilde{v}_i(t, \epsilon_2, \epsilon_3)$, and the first order Taylor expansion about ϵ_2 and ϵ_3 yields

$$\begin{aligned} \tilde{s}_i(t, \epsilon_2, \epsilon_3) &= \tilde{s}_{i,1}(t) + \epsilon_2 \tilde{s}_{i,2}(t) + \epsilon_3 \tilde{s}_{i,3}(t)\,, \\ \tilde{v}_i(t, \epsilon_2, \epsilon_3) &= \tilde{v}_{i,1}(t) + \epsilon_2 \tilde{v}_{i,2}(t) + \epsilon_3 \tilde{v}_{i,3}(t)\,. \end{aligned} \tag{22}$$

Indeed, according to (19), we have

$$\tilde{s}_{0,1}(t) = \frac{v_{\mathrm{amp}}}{\omega}\sin(\omega t)\,, \quad \tilde{v}_{0,1}(t) = v_{\mathrm{amp}}\cos(\omega t)\,, \tag{23}$$

while $\tilde{s}_{0,2}(t) = \tilde{s}_{0,3}(t) = 0$ and $\tilde{v}_{0,2}(t) = \tilde{v}_{0,3}(t) = 0$. Substituting (22) into (21) and matching the coefficients of ϵ_2 and ϵ_3 gives

$$\begin{aligned}
\dot{\tilde{s}}_{i,q}(t) &= \tilde{v}_{i,q}(t)\,,\\
\dot{\tilde{v}}_{i,q}(t) &= -\varphi_1^*\tilde{s}_{i,q}(t-\xi) - \kappa_1\tilde{v}_{i,q}(t-\xi)\\
&\quad + \varphi_1^*\tilde{s}_{i-1,q}(t-\xi) + \beta_1\tilde{v}_{i-1,q}(t-\xi)\\
&\quad + \alpha_1\lambda_q\big(\tilde{s}_{i-1,1}(t-\xi) - \tilde{s}_{i,1}(t-\xi)\big)^q\\
&\quad + \sum_{j=p}^{i-2}\Big[-\varphi_{i-j}^*\tilde{s}_{i,q}(t-\sigma) - \kappa_{i-j}\tilde{v}_{i,q}(t-\sigma)\\
&\qquad + \varphi_{i-j}^*\tilde{s}_{j,q}(t-\sigma) + \beta_{i-j}\tilde{v}_{j,q}(t-\sigma)\\
&\qquad + \sum_{j=p}^{i-2}\alpha_{i-j}\lambda_q\Big(\frac{\tilde{s}_{j,1}(t-\sigma) - \tilde{s}_{i,1}(t-\sigma)}{i-j}\Big)^q\Big]\,,
\end{aligned} \tag{24}$$

where $i = 1, 2, \ldots$, $q = 1, 2, 3$, $\lambda_1 = 0$ and $\lambda_2 = \lambda_3 = 1$.

For $q = 1$, (24) becomes a linear time-invariant (LTI) system with excitation arising only from $\tilde{s}_{0,1}(t)$ and $\tilde{v}_{0,1}(t)$; cf. (23). Thus, the steady states of (24) for $q = 1$ can be expressed by

$$\begin{aligned}
\tilde{s}_{is,1}(t) &= a_{i,1}\cos(\omega t) + b_{i,1}\sin(\omega t)\,,\\
\tilde{v}_{is,1}(t) &= c_{i,1}\cos(\omega t) + d_{i,1}\sin(\omega t)\,,
\end{aligned} \tag{25}$$

where $a_{i,1}, b_{i,1}, c_{i,1}, d_{i,1}$ are constant coefficients to be determined. For compactness, we collect them in the vector

$$z_{i,1} = [\, a_{i,1}\ b_{i,1}\ c_{i,1}\ d_{i,1}\,]^{\mathrm{T}}\,. \tag{26}$$

Substituting (25) into (24) for $q = 1$ and matching coefficients of $\cos(\omega t)$ and $\sin(\omega t)$, we obtain

$$z_{i,1} = \big(C(\omega)\big)^{-1}D_{i,1}\,, \tag{27}$$

where

$$\begin{aligned}
C(\omega) &= \begin{bmatrix} \omega E & -I_2 \\ C_{2,1}(\omega) & C_{2,2}(\omega)\end{bmatrix}\,,\\
D_{i,1} &= B_1^*\otimes F(\omega\xi)z_{i-1,1} + \sum_{j=p}^{i-2}B_{i-j}^*\otimes F(\omega\sigma)z_{j,1}\,.
\end{aligned} \tag{28}$$

Here, the operation $\otimes$ denotes the Kronecker product, I_2 denotes the 2-dimensional identity matrix, $B_{i-j}^* = B_{i-j}(h^*)$ is given in (11), and

$$\begin{aligned}
E &= \begin{bmatrix} 0 & 1\\ -1 & 0\end{bmatrix}\,,\quad F(\theta) = \begin{bmatrix}\cos\theta & -\sin\theta\\ \sin\theta & \cos\theta\end{bmatrix}\,,\\
C_{2,1}(\omega) &= \varphi_1 F(\omega\xi) + \sum_{j=p}^{i-2}\varphi_{i-j}F(\omega\sigma)\,,\\
C_{2,2}(\omega) &= \omega E + \kappa_1 F(\omega\xi) + \sum_{j=p}^{i-2}\kappa_{i-j}F(\omega\sigma)\,.
\end{aligned} \tag{29}$$

When considering (24) for $q = 2$ and $q = 3$, the whole network can be seen as a LTI system with external excitations only arising from $\tilde{s}_{j,1}^2$ and $\tilde{s}_{j,1}^3$ for $j = p, \ldots, i$, respectively. According to (25), $\tilde{s}_{j,1}^2$ only contains the frequency 2ω while $\tilde{s}_{j,1}^3$ contains frequencies ω and 3ω. Thus, the corresponding steady states can be written in the form

$$\begin{aligned}
\tilde{s}_{is,2}(t) &= a_{i,2}\cos(2\omega t) + b_{i,2}\sin(2\omega t)\,,\\
\tilde{v}_{is,2}(t) &= c_{i,2}\cos(2\omega t) + d_{i,2}\sin(2\omega t)\,,\\
\tilde{s}_{is,3}(t) &= a_{i,3,1}\cos(\omega t) + b_{i,3,1}\sin(\omega t)\\
&\quad + a_{i,3,3}\cos(3\omega t) + b_{i,3,3}\sin(3\omega t)\,,\\
\tilde{v}_{is,3}(t) &= c_{i,3,1}\cos(\omega t) + d_{i,3,1}\sin(\omega t)\\
&\quad + c_{i,3,3}\cos(3\omega t) + d_{i,3,3}\sin(3\omega t)\,.
\end{aligned} \tag{30}$$

We define coefficient vectors

$$\begin{aligned}
z_{i,2} &= [\, a_{i,2}\ b_{i,2}\ c_{i,2}\ d_{i,2}\,]^{\mathrm{T}}\,,\\
z_{i,3,k} &= [\, a_{i,3,k}\ b_{i,3,k}\ c_{i,3,k}\ d_{i,3,k}\,]^{\mathrm{T}}\,,\quad k = 1, 3\,,
\end{aligned} \tag{31}$$

cf. (26). Substituting (30) into (24) for $q = 2$ and $q = 3$, one can obtain the coefficients

$$\begin{aligned}
z_{i,2} &= \big(C(2\omega)\big)^{-1}D_{i,2}\,,\\
z_{i,3,k} &= \big(C(k\omega)\big)^{-1}D_{i,3,k}\,,\quad k = 1, 3\,,
\end{aligned} \tag{32}$$

where the matrix C is defined in (28,29) and

$$\begin{aligned}
D_{i,2} &= B_1^*\otimes F(2\omega\xi)z_{i-1,2} + \sum_{j=p}^{i-2}B_{i-j}^*\otimes F(2\omega\sigma)z_{j,2}\\
&\quad + \alpha_1 M(2\omega\xi)J_{i-1} + \sum_{j=p}^{i-2}\frac{\alpha_{i-j}}{(i-j)^2}M(2\omega\sigma)J_j\,,\\
D_{i,3,k} &= B_1^*\otimes F(k\omega\xi)z_{i-1,3,k} + \sum_{j=p}^{i-2}B_{i-j}^*\otimes F(k\omega\sigma)z_{j,3,k}\\
&\quad + \alpha_1 M(k\omega\xi)K_{i-1,k} + \sum_{j=p}^{i-2}\frac{\alpha_{i-j}}{(i-j)^3}M(k\omega\sigma)K_{j,k}\,,
\end{aligned} \tag{33}$$

for $k = 1, 3$, and

$$\begin{aligned}
M(\theta) &= \begin{bmatrix} O_2 & O_2\\ O_2 & F(\theta)\end{bmatrix}\,,\\
J_j &= \begin{bmatrix} 0\\ 0\\ \big((a_{j,1}-a_{i,1})^2 - (b_{j,1}-b_{i,1})^2\big)/2\\ (a_{j,1}-a_{i,1})(b_{j,1}-b_{i,1})\end{bmatrix}\,,\\
K_{j,1} &= \begin{bmatrix} 0\\ 0\\ \big(3(a_{j,1}-a_{i,1})^3 + 3(a_{j,1}-a_{i,1})(b_{j,1}-b_{i,1})^2\big)/4\\ \big(3(a_{j,1}-a_{i,1})^2(b_{j,1}-b_{i,1}) + 3(b_{j,1}-b_{i,1})^3\big)/4\end{bmatrix}\,,\\
K_{j,3} &= \begin{bmatrix} 0\\ 0\\ \big((a_{j,1}-a_{i,1})^3 - 3(a_{j,1}-a_{i,1})(b_{j,1}-b_{i,1})^2\big)/4\\ \big(3(a_{j,1}-a_{i,1})^2(b_{j,1}-b_{i,1}) - (b_{j,1}-b_{i,1})^3\big)/4\end{bmatrix}\,,
\end{aligned} \tag{34}$$

and O_2 denotes the 2-dimensional zero matrix.

According to (22), we can approximate the steady states $\tilde{s}_{is}(t)$ and $\tilde{v}_{is}(t)$ by using the solutions (25) and (30) for all $i = 1, \ldots, n$. Then, one can use the condition (20) to evaluate the head-to-tail string stability of a vehicle network.

4. CASE STUDY AND SIMULATIONS

In this section, we investigate the dynamics of a 31-vehicle network where every other vehicle monitors the second nearest vehicle using communication, as shown in Fig. 2. We assume that all vehicles are driven by human drivers with reaction time $\tau = 0.5$ [s] and the control gains $\alpha_1 = 0.3$ [1/s], $\beta_1 = 0.5$ [1/s]. We also assume the communication delay $\sigma = 0.2$ [s]. Then, we design α_2 and β_2 to achieve plant stability for CCC vehicles and to guarantee head-to-tail string stability. For plant stability, we use Theorem 2 and consider $\mathcal{D} = \{h : 13 \le h \le 27\ [\mathrm{m}]\}$ that corresponds to the velocity range $4.96 \lesssim v \lesssim 25.04$ [m/s]. We remark that the plant stable domain decreases when the area of $\mathcal{D}$ enlarges. However, since Theorem 2 is a sufficient condition, the obtained control gains may also result in plant stability for a domain larger than $\mathcal{D}$. To test head-to-tail string

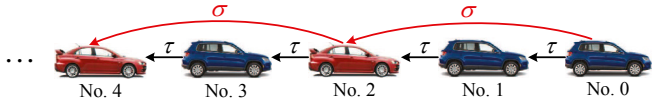

Fig. 2. Connected vehicle system with next-nearest neighbor interactions. Symbols τ and σ denote the human reaction time and communication delay, respectively.

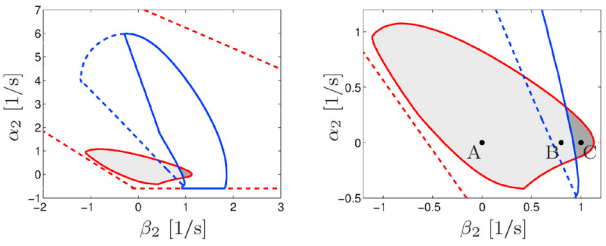

Fig. 3. Stability diagram for a 31-vehicle network with configuration shown in Fig. 2. The right panel is a zoomed region of the left panel. The plant stable domain and the string stable domain are shaded by light gray and dark gray, respectively. Solid red and solid blue curves denote the plant stability and string stability boundaries, respectively. The dashed counterparts are the stability boundaries obtained based on the linearized model.

stability, we use the condition (20) with $v^* = 22.5$ [m/s] and $v_{\rm amp} = 6$ [m/s]; cf. (19). The corresponding stability diagram is shown in the (β_2, α_2)-plane in Fig. 3, where the plant stable domain and the string stable domain are shaded by light gray and dark gray, respectively. The solid red and the solid blue curves denote the plant stability boundary and string stability boundary, respectively, while the dashed red and the dashed blue curves are the boundaries obtained by Zhang and Orosz (2015a) based on the linearized model.

To demonstrate the system performance, we use the control gains corresponding to the points A–C shown in the right panel of Fig. 3. Simulations shown in Fig. 4(a)–(c) indicate that the system is plant stable for these three cases. Point A ($\alpha_2 = \beta_2 = 0$) represents the case when the communication is not utilized, and this point is outside the linear and nonlinear string stable domains. Correspondingly, Fig. 4(a) demonstrates that the disturbance arising from the head vehicle is amplified when reaching the tail vehicle and leads to stop-and-go motion. Point B is inside the linear string stable domain but outside the nonlinear one, and Fig. 4(b) shows that the disturbance is amplified; see the zoomed region. Point C is inside the nonlinear string stable domain and thus the disturbances are attenuated as shown in Fig. 4(c); see the zoomed region. All simulations show that the steady state of the tail vehicle is periodic with the same period as the head vehicle, although the oscillations are not sinusoidal. In Fig. 4(d), for case B we compare the linear estimation (dashed red) obtained in Zhang and Orosz (2015a) and nonlinear estimation (dashed blue) obtained by using the method given in Section 3.2, where the numerical simulation (solid black) of the tail vehicle is given as benchmark. It shows that the nonlinear estimation is more accurate than the linear estimation, especially close at the peak value, which corresponds to the $\mathcal{L}_\infty$ norm of the signal.

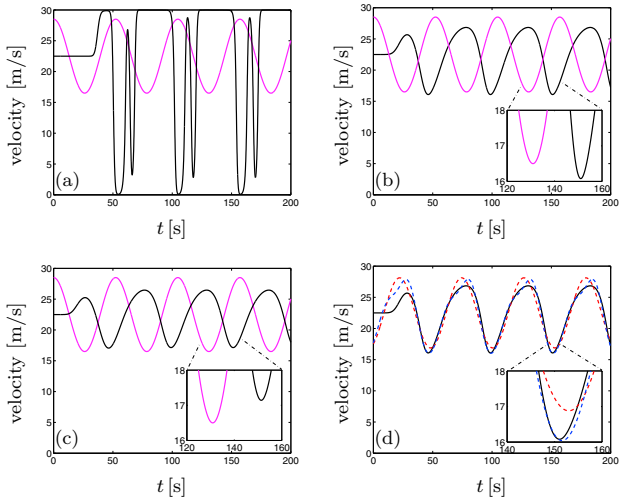

Fig. 4. Simulations for points A–C in Fig. 3 are shown in panels (a)–(c), respectively, where the velocities of head vehicle and tail vehicle are plotted by the magenta and the black curves, respectively. Panel (d) demonstrates the comparison of the linear estimation (red dashed) and the nonlinear estimation (blue dashed) with the numerical simulation (black solid) of the tail vehicle for case B.

5. CONCLUSION

In this paper, we investigated the dynamics of nonlinear connected vehicle systems in presence of information delays. Sufficient conditions for plant stability and head-to-tail string stability were derived based on Lyapunov-Krasovskii theory and then visualized in stability diagrams for choosing control gains. Numerical simulations indicated that the stable domains derived in this paper are more accurate than the ones obtained by using linearized models. In our CCC design, we neglected some physical effects such as air drag and rolling resistance. In the future, we will investigate the design of CCC based on physics-based vehicle models.

REFERENCES

Ge, J.I. and Orosz, G. (2014). Dynamics of connected vehicle systems with delayed acceleration feedback. *Transportation Research Part C*, 46, 46–64.

Johansson, G. and Rumar, K. (1971). Drivers' brake reaction times. *Human Factors*, 13(1), 23–27.

Milanes, V., Shladover, S.E., Spring, J., Nowakowski, C., Kawazoe, H., and Nakamura, M. (2014). Cooperative adaptive cruise control in real traffic situations. *IEEE Transactions on Intelligent Transportation Systems*, 15(1), 296–305.

Orosz, G. (2014). Connected cruise control: modeling, delay effects, and nonlinear behavior. *Vehicle System Dynamics,*, submitted.

Orosz, G., Wilson, R.E., and Stépán, G. (2010). Traffic jams: dynamics and control. *Philosophical Transactions of the Royal Society A*, 368(1928), 4455–4479.

Ploeg, J., Shukla, D.P., van de Wouw, N., and Nijmeijer, H. (2014). Controller synthesis for string stability of vehicle platoons. *IEEE Transactions on Intelligent Transportation Systems*, 15(2), 854–865.

Qin, W.B., Gomez, M.M., and Orosz, G. (2014). Stability analysis of connected cruise control with stochastic delays. In *American Control Conference*, 5534–5539.

Zhang, L. and Orosz, G. (2013). Designing network motifs in connected vehicle systems: delay effects and stability. In *Proceedings of the ASME Dynamic Systems and Control Conference*, DSCC2013-4081, V003T42A006.

Zhang, L. and Orosz, G. (2015a). Motif-based design for connected vehicle systems in presence of heterogeneous connectivity structures and time delays. *IEEE Transactions on Intelligent Transportation Systems*, (submitted).

Zhang, L. and Orosz, G. (2015b). Nonlinear connected vehicle system with communication delays. In *American Control Conference*, (accepted).

Zhao, Y., Minero, P., and Gupta, V. (2014). On disturbance propagation in leader-follower systems with limited leader information. *Automatica*, 50, 591–598.

Appendix A. PROOF OF THEOREM 2

When analyzing plant stability, we neglect the disturbances from other vehicles, i.e., $\tilde{x}_j(t) \equiv 0$ for $j = p, \dots, i-1$ in (10), leading to

$$\dot{\tilde{x}}_i(t) = A_0\tilde{x}_i(t) + A_{\xi,i}\tilde{x}_i(t-\xi) + A_{\sigma,i}\tilde{x}_i(t-\sigma)\,. \quad \text{(A.1)}$$

Using Newton-Leibniz formula

$$\tilde{x}_i(t-\xi) = \tilde{x}_i(t) - \int_{t-\xi}^{t} \dot{\tilde{x}}_i(\rho)\,\mathrm{d}\rho \quad \text{(A.2)}$$

in (A.1) results in

$$\dot{\tilde{x}}_i(t) = A_i\tilde{x}_i(t) - A_{\mathrm{d},i}\int_{t-\sigma}^{t} \dot{\tilde{x}}_i(\rho)\,\mathrm{d}\rho - A_{\xi,i}\int_{t-\xi}^{t-\sigma} \dot{\tilde{x}}_i(\rho)\,\mathrm{d}\rho\,. \quad \text{(A.3)}$$

To investigate the stability of the equilibrium (4) for $\xi \neq \sigma$, we use the functional

$$\begin{aligned} L &= \tilde{x}_i^{\mathrm{T}}(t)P\tilde{x}_i(t) + \int_{t-\xi}^{t} \tilde{x}_i^{\mathrm{T}}(\rho)Q_1\tilde{x}_i(\rho)\,\mathrm{d}\rho \\ &+ \int_{t-\sigma}^{t} \tilde{x}_i^{\mathrm{T}}(\rho)Q_2\tilde{x}_i(\rho)\,\mathrm{d}\rho + \int_{-\sigma}^{0}\int_{t+\theta}^{t} \dot{\tilde{x}}_i^{\mathrm{T}}(\rho)W_1\dot{\tilde{x}}_i(\rho)\,\mathrm{d}\rho\mathrm{d}\theta \\ &+ \mathrm{sgn}(\xi-\sigma)\int_{-\xi}^{-\sigma}\int_{t+\theta}^{t} \dot{\tilde{x}}_i^{\mathrm{T}}(\rho)W_2\dot{\tilde{x}}_i(\rho)\,\mathrm{d}\rho\mathrm{d}\theta\,, \end{aligned} \quad \text{(A.4)}$$

where the constant matrices P, Q_1, Q_2, W_1, W_2 are all positive definite so that L is positive definite as well.

Differentiating (A.4) with respect to time, substituting (A.1) and (A.3) into the result, and adding

$$0 = |\xi-\sigma|x_i^{\mathrm{T}}(t)Rx_i(t) - \mathrm{sgn}(\xi-\sigma)\int_{t-\xi}^{t-\sigma} x_i^{\mathrm{T}}(t)Rx_i(t)\,\mathrm{d}\rho \quad \text{(A.5)}$$

to the resulting equation, we obtain

$$\begin{aligned} \dot{L} &= \tilde{X}_i^{\mathrm{T}}(t)\Phi\tilde{X}_i(t) - 2\tilde{x}_i^{\mathrm{T}}(t)PA_{\mathrm{d},i}\int_{t-\sigma}^{t} \dot{\tilde{x}}_i(\rho)\,\mathrm{d}\rho \\ &- 2\tilde{x}_i^{\mathrm{T}}(t)PA_{\xi,i}\int_{t-\xi}^{t-\sigma} \dot{\tilde{x}}_i(\rho)\,\mathrm{d}\rho - \int_{t-\sigma}^{t} \dot{\tilde{x}}_i^{\mathrm{T}}(\rho)W_1\dot{\tilde{x}}_i(\rho)\,\mathrm{d}\rho \\ &- \mathrm{sgn}(\xi-\sigma)\int_{t-\xi}^{t-\sigma} \tilde{x}_i^{\mathrm{T}}(\rho)W_2\dot{\tilde{x}}_i(\rho)\,\mathrm{d}\rho\,. \end{aligned} \quad \text{(A.6)}$$

Here, $\tilde{X}_i^{\mathrm{T}}(t) = [\tilde{x}_i^{\mathrm{T}}(t),\ \tilde{x}_i^{\mathrm{T}}(t-\xi),\ \tilde{x}_i^{\mathrm{T}}(t-\sigma)]$ and

$$\Phi = \begin{bmatrix} H_2 & A_0^{\mathrm{T}}H_1A_{\xi,i} & A_0^{\mathrm{T}}H_1A_{\sigma,i} \\ A_{\xi,i}^{\mathrm{T}}H_1A_0 & A_{\xi,i}^{\mathrm{T}}H_1A_{\xi,i} - Q_1 & A_{\xi,i}^{\mathrm{T}}H_1A_{\sigma,i} \\ A_{\sigma,i}^{\mathrm{T}}H_1A_0 & A_{\sigma,i}^{\mathrm{T}}H_1A_{\xi,i} & A_{\sigma,i}^{\mathrm{T}}H_1A_{\sigma,i} - Q_2 \end{bmatrix}, \quad \text{(A.7)}$$

where H_1 and H_2 are given in (17). Substituting the identity

$$\tilde{X}_i^{\mathrm{T}}(t)\Phi\tilde{X}_i(t) = \frac{1}{\sigma}\int_{t-\sigma}^{t} \tilde{X}_i^{\mathrm{T}}(t)\Phi\tilde{X}_i(t)\,\mathrm{d}\rho \quad \text{(A.8)}$$

into (A.6) leads to

$$\dot{L} = \int_{t-\sigma}^{t} \tilde{\chi}_i^{\mathrm{T}}(t,\rho)\Xi_1\tilde{\chi}_i(t,\rho)\,\mathrm{d}\rho + \int_{t-\xi}^{t-\sigma} \tilde{\phi}_i^{\mathrm{T}}(t,\rho)\Xi_2\tilde{\phi}_i(t,\rho)\,\mathrm{d}\rho\,, \quad \text{(A.9)}$$

where $\tilde{\chi}_i^{\mathrm{T}}(t,\rho) = [\tilde{x}_i^{\mathrm{T}}(t),\ \tilde{x}_i^{\mathrm{T}}(t-\xi),\ \tilde{x}_i^{\mathrm{T}}(t-\sigma),\ \dot{\tilde{x}}_i^{\mathrm{T}}(\rho)]$, $\tilde{\phi}_i^{\mathrm{T}}(t,\rho) = [\tilde{x}_i^{\mathrm{T}}(t),\ \dot{\tilde{x}}_i^{\mathrm{T}}(\rho)]$, and Ξ_1, Ξ_2 are given in (16). Indeed, both matrices Ξ_1 and Ξ_2 depend on $\Psi_i \in \mathcal{D}^{i-p}$; cf. (11) and (13). If Ξ_1 and Ξ_2 are both negative definite over the whole domain $\mathcal{D}^{i-p}$, then $\dot{L}$ is negative definite for $\forall\Psi_i \in \mathcal{D}^{i-p}$, implying $\tilde{x}_i(t) \to 0$ as $t \to \infty$.

Appendix B. PROOF OF THEOREM 3

First, we study the dynamics of vehicle i and assume that the states of vehicle $j = p, \dots, i-1$ are T-periodic, i.e.,

$$s_j(t+T) = s_j(t)\,, \quad v_j(t+T) = v_j(t)\,. \quad \text{(B.1)}$$

We define the error states as $e_{i,s}(t) = s_i(t+T) - s_i(t)$ and $e_{i,v}(t) = v_i(t+T) - v_i(t)$. Then, substituting $t = t+T$ into (1) and subtracting (1) from the result while considering (B.1) results in

$$\begin{aligned} \dot{e}_{i,s}(t) &= e_{i,v}(t)\,, \\ \dot{e}_{i,v}(t) &= \alpha_1\big(V\big(h_{i,i-1}(t+T-\xi)\big) - V\big(h_{i,i-1}(t-\xi)\big)\big) \\ &+ \sum_{j=p}^{i-2}\alpha_{i-j}\big(V\big(h_{i,j}(t+T-\sigma)\big) - V\big(h_{i,j}(t-\sigma)\big)\big) \\ &- \kappa_1 e_{i,v}(t-\xi) - \sum_{j=p}^{i-2}\kappa_{i-j}e_{i,v}(t-\sigma)\,, \end{aligned} \quad \text{(B.2)}$$

where κ_{i-j} is given in (12). For $h_{i,j} \in \mathcal{D}$, based on the mean value theorem, there exist variables $\mu_{i,j} \in \mathcal{D}$ such that

$$V\big(h_{i,j}(t+T-r)\big) - V\big(h_{i,j}(t-r)\big) = -\frac{V'(\mu_{i,j})}{i-j}e_{i,s}(t-r)\,, \quad \text{(B.3)}$$

where r can be either ξ or σ.

Substituting (B.3) into (B.2) and writing the result into matrix form leads to

$$\dot{e}_i(t) = A_0e_i(t) + A_{\xi,i}(U_i)e_i(t-\xi) + A_{\sigma,i}(U_i)e_i(t-\sigma)\,, \quad \text{(B.4)}$$

where $e_i(t) = [e_{i,s}(t)\,, e_{i,v}(t)]^{\mathrm{T}}$, $U_i = [\mu_{i,i-1}, \dots, \mu_{i,p}]$, and A_0, $A_{\xi,i}$, $A_{\sigma,i}$ are given in (11) by replacing Ψ_i with U_i.

Note that (B.4) is analogous to (A.1) since Ψ_i and U_i have the same bounds, i.e., $\Psi_i, U_i \in \mathcal{D}^{i-p}$. When Theorem 1 and Theorem 2 hold, the equilibrium $\tilde{x}_i(t) = 0$ is asymptotically stable in (A.1). Analogously, if Theorem 1 and Theorem 2 hold, $e_i(t) = 0$ is asymptotically stable in (B.4) as well. At steady state, we have $e_{is}(t) = 0$, implying that $x_{is}(t+T) = x_{is}(t)$.

Since the state of vehicle 0 is T-periodic, the steady-state of vehicle 1 will be T-periodic. Repeating this process to vehicles $i = 2, 3, \dots$ completes the proof.